

# Imbalanced initial populations between dark and bright states in semiconductor quantum dots

Sheng-Di Lin,<sup>\*</sup> Ying-Jhe Fu, and Chun Cheng

Department of Electronics Engineering, National Chiao Tung University, 1001 University Road, Hsinchu 300, Taiwan

<sup>\*</sup>sdlin@mail.nctu.edu.tw

**Abstract:** We present the observation and analysis of long-lived exciton in individual InAs quantum dots (QDs). The general model considering the interplay between dark and bright states reveals the two key factors responsible for the long decay time: the shortened spin-flip time at elevated temperature and the imbalanced initial populations between the dark and bright states. The later one plays a key role in the unusual phenomena and leads to the possibility of spin-dependent relaxation process in QDs.

©2012 Optical Society of America

**OCIS codes:** (300.6500) Spectroscopy, time-resolved; (320.7130) Ultrafast processes in condensed matter, including semiconductors.

---

## References and links

1. D. J. Mowbray and M. S. Skolnick, "New physics and devices based on self-assembled semiconductor quantum dots," *J. Phys. D Appl. Phys.* **38**(13), 2059–2076 (2005).
2. A. J. Ramsay, "A review of the coherent optical control of the exciton and spin states of semiconductor quantum dots," *Semicond. Sci. Technol.* **25**(10), 103001 (2010).
3. C. H. Wu, Y. G. Lin, S. L. Tyan, S. D. Lin, and C. P. Lee, "An investigation of quantum states in ultra-small InAs-GaAs quantum dots by means of photoluminescence," *Chin. J. Physiol.* **43**, 847–855 (2005).
4. A. Imamoğlu, D. D. Awschalom, G. Burkard, D. P. DiVincenzo, D. Loss, M. Sherwin, and A. Small, "Quantum information processing using quantum dot spins and cavity QED," *Phys. Rev. Lett.* **83**(20), 4204–4207 (1999).
5. O. Labeau, P. Tamarat, and B. Lounis, "Temperature dependence of the luminescence lifetime of single CdSe/ZnS quantum dots," *Phys. Rev. Lett.* **90**(25), 257404 (2003).
6. J. M. Smith, P. A. Dalgarno, R. J. Warburton, A. O. Govorov, K. Karrai, B. D. Gerardot, and P. M. Petroff, "Voltage control of the spin dynamics of an exciton in a semiconductor quantum dot," *Phys. Rev. Lett.* **94**(19), 197402 (2005).
7. M. Bayer, G. Ortner, O. Stern, A. Kuther, A. A. Gorbunov, A. Forchel, P. Hawrylak, S. Fafard, K. Hinzer, T. L. Reinecke, S. N. Walck, J. P. Reithmaier, F. Kloppe, and F. Schäfer, "Fine structure of neutral and charged excitons in self-assembled In(Ga)As/(Al)GaAs quantum dots," *Phys. Rev. B* **65**(19), 195315 (2002).
8. T. Kümmell, S. V. Zaitsev, A. Gust, C. Kruse, D. Hommel, and G. Bacher, "Radiative recombination in photoexcited quantum dots up to room temperature: the role of fine-structure effects," *Phys. Rev. B* **81**(24), 241306 (2010).
9. J. Johansen, B. Julsgaard, S. Stobbe, J. M. Hvam, and P. Lodahl, "Probing long-lived dark excitons in self-assembled quantum dots," *Phys. Rev. B* **81**(8), 081304 (2010).
10. C. Cheng, S. D. Lin, C. H. Pan, C. H. Lin, and Y. J. Fu, "Observation of long-lived excitons in InAs quantum dots under thermal redistribution temperature," *Phys. Lett. A* **376**(17), 1495–1498 (2012).
11. W. Yang, R. R. Lowe-Webb, H. Lee, and P. C. Sercel, "Effect of carrier emission and retrapping on luminescence time decays in InAs-GaAs quantum dots," *Phys. Rev. B* **56**(20), 13314–13320 (1997).
12. S. Sanguinetti, M. Henini, M. Grassi Alessi, M. Capizzi, P. Frigeri, and S. Franchi, "Carrier thermal escape and retrapping in self-assembled quantum dots," *Phys. Rev. B* **60**(11), 8276–8283 (1999).
13. G. Wang, S. Fafard, D. Leonard, J. E. Bowers, J. L. Merz, and P. M. Petroff, "Time-resolved optical characterization of InGaAs/GaAs quantum dots," *Appl. Phys. Lett.* **64**(21), 2815–2817 (1994).
14. D. I. Lubyshev, P. P. Gonzalez-Borrero, E. Marega, Jr., E. Petitprez, N. La Scala, Jr., and P. Basmaji, "Exciton localization and temperature stability in self-organized InAs quantum dots," *Appl. Phys. Lett.* **68**(2), 205–207 (1996).
15. H. Yu, S. Lycett, C. Roberts, and R. Murray, "Time resolved study of self-assembled InAs quantum dots," *Appl. Phys. Lett.* **69**(26), 4087–4089 (1996).
16. C. H. Lin, H. S. Lin, C. C. Huang, S. K. Su, S. D. Lin, K. W. Sun, C. P. Lee, Y. K. Liu, M. D. Yang, and J. L. Shen, "Temperature dependence of time-resolved photoluminescence spectroscopy in InAs/GaAs quantum ring," *Appl. Phys. Lett.* **94**(18), 183101 (2009).
17. M. Paillard, X. Marie, P. Renucci, T. Amand, A. Jbeli, and J. M. Gérard, "Spin relaxation quenching in semiconductor quantum dots," *Phys. Rev. Lett.* **86**(8), 1634–1637 (2001).

18. Y. H. Liao, J. I. Climente, and S. J. Cheng, "Dominant channels of exciton spin relaxation in photoexcited self-assembled (In,Ga)As quantum dots," *Phys. Rev. B* **83**(16), 165317 (2011).
19. B. Patton, W. Langbein, and U. Woggon, "Trion, biexciton, and exciton dynamics in single self-assembled CdSe quantum dots," *Phys. Rev. B* **68**(12), 125316 (2003).
20. G. A. Narvaez, G. Bester, A. Franceschetti, and A. Zunger, "Excitonic exchange effects on the radiative decay time of monoexcitons and biexcitons in quantum dots," *Phys. Rev. B* **74**(20), 205422 (2006).
21. P. Maletinsky, C. W. Lai, A. Badolato, and A. Imamoglu, "Nonlinear dynamics of quantum dot nuclear spins," *Phys. Rev. B* **75**(3), 035409 (2007).

## 1. Introduction

In the past two decades, self-assembled semiconductor quantum dots (QDs) have been a central topic in the field of nano-photonics and quantum information science. Thanks to their defect-free quality and superior optical properties, the applications on optoelectronic devices and quantum information processing grow rapidly in these years [1–3]. The single electron-hole pair forms in a QD, named as exciton, can be divided into two kinds: bright (optically active) and dark (optically inactive) excitons due to their spin orientations. Although the bright exciton is preferred for optical sensing and emission, the dark excitons received growing attention for their possible use in spin storage and qubits [4–6]. In this aspect, it is essential to understand the interplay between bright and dark excitons and quite a few works have been done very recently [5–9]. Additionally, the long-lived exciton in individual InAs QDs below thermal redistribution temperature was observed by us [10], which is triggered by the thermal-induced spin flip which turns dark excitons into bright ones. In this paper, we analyze this issue in a more general way and it leads to a conclusion of that, the very long decay time of bright exciton comes from the imbalanced initial population of excitons between bright and dark states. This conclusion indicates the possibility of spin-dependent relaxation process of carriers in QDs, which is interesting to researchers in the field of spin-related physics and also of importance for spin storage application.

To experimentally study the dynamics of bright excitons in QDs, temperature-dependent time-resolved photoluminescence (TRPL) is one of the most common methods [8–16]. Although the temperature-dependent decay times of bright exciton in InAs QDs ensembles has been extensively studied, its physical mechanism in whole temperature range is still under debate [8]. Regarding to the dark excitons in QDs, as they are optically inactive, to probe them in optical means is much more difficult. By applying in-plane magnetic field on QDs, it is possible to couple dark states with bright ones [7] so they can be probed directly. To investigate dark states without disturbing them, one has to develop a model describing the interplay between dark and other states, such as bright states or traps [5, 8, 9]. With the help of model simulation, the properties of dark states can be revealed experimentally.

In this report, we first present the time traces of TRPL measurement on two representative samples, a regular one and the other one with very long decay time. To understand the cause of the unusual long decay time, we perform the power dependence of TRPL and it shows that the long decay time comes from the fastened spin-flip of dark excitons. With the discussion on the analytical solution of a general model, in which the spin-flip time between dark and bright states is temperature-dependent, we conclude that, to explain the unusual behavior, the initial population of dark states has to be at least two-fold higher than that of bright states. This leads to the possibility of spin-dependent relaxation process in QDs. The sample dependence of the unusual behavior has also been discussed.

## 2. Sample growth and measurement setup

On (100) GaAs substrates, more than twenty samples grown by a solid-source molecular beam epitaxy (MBE) system are studied. For clarity, we present six selected samples here, noted as sample S1 to S6. The QDs were centrally embedded in GaAs and sandwiched with two AlGaAs confinement layers. The growth ended with an uncapped QDs layer grown at the same condition for surface morphology observation with atomic force microscopy in air. In Table 1, we summarize the basic parameters of QDs, including the growth temperature, the InAs nominal thickness, the area density, the PL peak energy and the full-width-half-maxima

(FWHM) of the PL spectra take at 20 K. Note that, from sample S1 to S6, the PL peak energies (that is, the ground state energy of QDs) increase from 1.08 to 1.30 eV.

**Table 1. The growth conditions and basic parameters of the six QD samples.**

Sample number	QDs' growth temperature (°C)	InAs thickness (MLs)	QDs' area density ( $10^{10}/\text{cm}^2$ )	PL peak energy (eV)	PL FWHM (meV)
S1 (LM4682)	500	3.0	6.0	1.08	33
S2 (LM4681)	500	2.4	6.8	1.15	95
S3 (LM3572)	480	2.4	8.2	1.20	92
S4 (LM3573)	480	2.4	13	1.25	70
S5 (LM3472)	480	2.6	4.5	1.27	57
S6 (LM4596)	480	2.0	2.8	1.30	97

For TRPL measurements, the samples were excited with a pulsed diode laser ( $\lambda = 780$  nm, pulse width  $\sim 50$  ps and repetition rate = 10 MHz) with a spot size of about  $60 \mu\text{m}$ . By considering the spot size and the net absorption of GaAs matrix, together with the QDs' density and excitation power, the number of photo-generated electron-hole pairs per dot can be estimated. The PL selected by a monochromator is detected by an InGaAs photo-multiplier tube (PMT) using time-correlated single photon counting technique. The time resolution of TRPL system is about 0.3 ns, limited by the response time of InGaAs PMT. At each temperature, the PL spectra were taken prior to the TRPL measurements to decide the detection wavelength. The PL decay time is extracted by fitting the measured decay curves with the bi-exponential function,  $I_{PL}(t) = A_1 \exp(-t/\tau_1) + A_2 \exp(-t/\tau_2)$ . In this report, we define the fast part of the decay curve as the PL decay time (i.e. the smaller  $\tau$ , denoted as  $\tau_1$ ).

### 3. Experimental results and discussion

#### 3.1 PL decay curves of samples S1 and S3

For clarity, we first show the TRPL results of the two representative samples, S1 and S3. In Fig. 1(a), we plot the measured time traces of sample S1 from 35 K to 75 K under the average excitation power of  $2 \mu\text{W}$ , which could generate about 0.18 e-h pairs per QD in each pulse. Note that the vertically-shifted PL intensity is plotted in logarithmic scale so their slopes are roughly proportional to the inverse of decay times. At the lowest temperature of 35 K, the nearly flat time traces after about 8 ns shows that it is basically a mono-exponential decay. As the temperatures increase from 45 K to 60 K, the slow part of the decay becomes more significant but it vanishes again when the temperatures go even higher to 75 K. It is worth mentioning that the decay curves can be fitted pretty well with the bi-exponential function stated above. The PL time traces of sample S3 showing in Fig. 1(b) have a very different trend in the same temperature range. At  $T = 35$  K, the slow part of the decay has been very clearly seen. With the increasing temperatures, the slow part substitutes the fast part at about 55 K, which makes the whole decay very slow. Such a clear difference is also revealed in Fig. 2 by plotting the extracted parameters  $\tau_1$ ,  $\tau_2$  and the  $A_2$  ratio that is defined as  $A_2/(A_1 + A_2)$ . To make the comparison easier, we have used the same scales in Fig. 2(a) and Fig. 2(b). For sample S1 (Fig. 2(a)), a typical result is obtained. That is, as the temperatures increase from 35 K to 85 K, the fast decay times  $\tau_1$  increase from about 0.6 ns to about 1.1 ns but the slow decay times  $\tau_2$ , which is commonly believed due to the slow spin-flip time of turning dark excitons into bright ones, decreases from more than 10 ns down to about 2.2 ns. This behavior has been observed by a few groups [5, 8, 9, 16, 17], which will be quantitatively discussed later in this paper by a general model. In Fig. 2(b), however, an unusual trend is seen in sample S3. At  $T = 55$  K, the fast decay part is taken over by the slow one so the  $\tau_1$  dramatically increases to about 7.5 ns. For  $T > 55$  K, the fast decay part vanishes so the whole decay curve become mono-exponential. Let us look at the  $A_2$  ratio dependence on temperature. For sample S1, the maximum of  $A_2$  ratio is less than 0.2, which, however, can be larger than 0.4 for sample S3. In all our measurements, a large value of  $A_2$  ratio is essential for the substitution to happen.

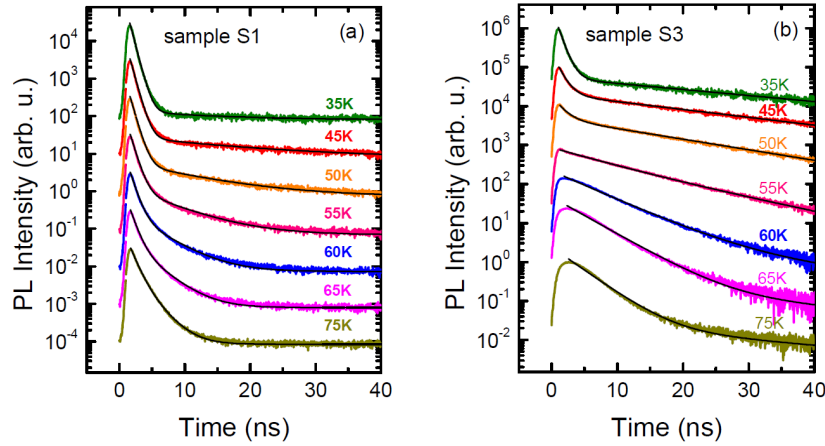


Fig. 1. The measured PL time traces of sample S1 (a) and S3 (b) at various temperatures. The bi-exponentially fitting curves are also plotted.

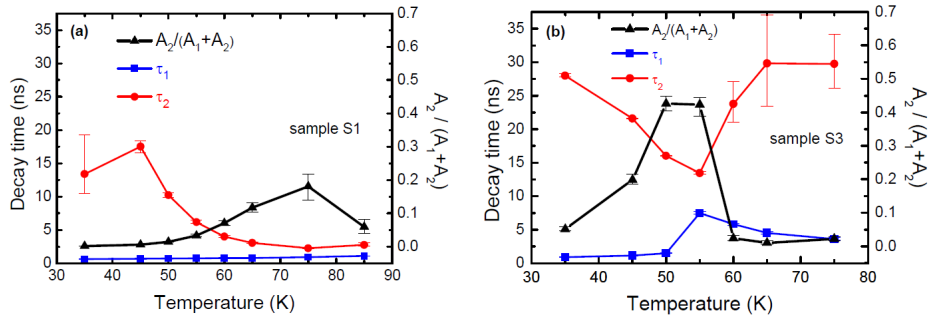


Fig. 2. The extracted bi-exponential decay times and  $A_2$  ratio of sample S1 (a) and S3 (b) at various temperatures.

To understand the source of the slow decay parts, we have performed power-dependent TRPL measurement on sample S3. In Fig. 3(a), the measured time traces at the excitation powers of 5 – 40  $\mu\text{W}$  are plotted, as well as the corresponding  $\tau_1$ ,  $\tau_2$  and  $A_2$  ratios in Fig. 3(b). With a careful look at the time traces of 5- $\mu\text{W}$  excitation power, one can clearly see that the fast decay is taken over by the slow one at 55 K, which is similar to that in Fig. 1(b). However, when the excitation power increases to 20 or 40  $\mu\text{W}$ , the substitution becomes unclear. This also illustrates with the extracted decay times and  $A_2$  ratios in Fig. 3(b). For the excitation power of 5, 10, 20, and 40  $\mu\text{W}$ , the maximum of  $\tau_1$  decreases from 6.0, 5.3, 4.2, to 2.7 ns. Meanwhile, the minimum of  $\tau_2$  also decreases from 13.9, 12.8, 11.6, to 8.8 ns and the maximum of  $A_2$  ratios decreases from 0.40, 0.34, 0.25, to 0.17. This power-dependent behavior can be qualitatively explained by considering the biexciton occupation probability among the ensemble of QDs. The increasing excitation power enhances the possibility of biexciton occupation in QDs. Note that, for sample S3, the excitation power of 40  $\mu\text{W}$  corresponds to about 2.6 e-h pair per QD per pulse. In a QD, because the biexciton decay generates a photon and leaves the exciton in bright state, the initial population of dark states is reduced. As a result, the slow decay arising from the spin-flip of dark excitons has little chance to replace the fast one when the temperature increases. A quantitative discussion on the role of the initial population of dark states will be given later in this paper.

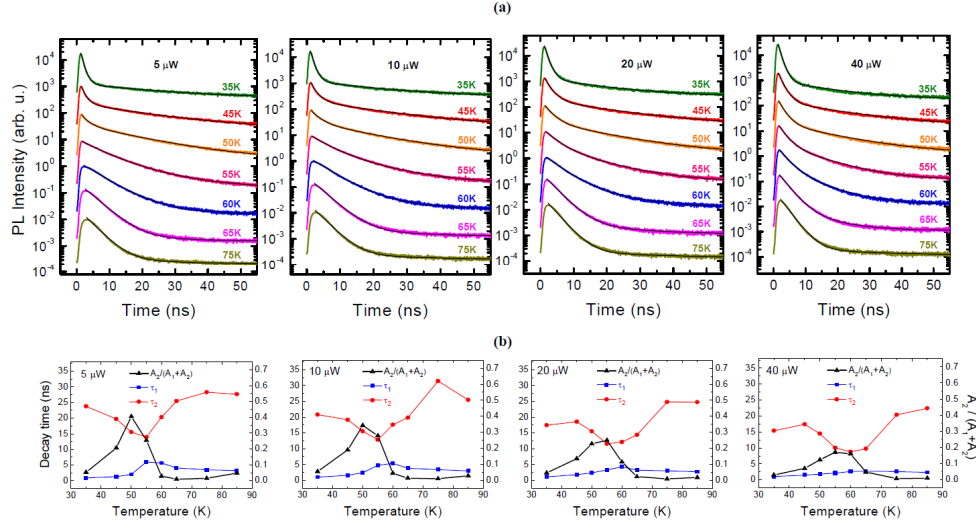


Fig. 3. The measured time traces of sample S3 under various excitation powers (a), and their extracted bi-exponential decay times and  $A_2$  ratio (b) at various temperatures.

### 3.2 Theoretical model and discussion

To explain the unusual behavior quantitatively, we consider a general model including the bright, dark and empty states in QDs, as shown in Fig. 4. In this model of excitonic states, three levels including bright, dark and empty states are included. The energy difference between bright and dark excitonic states ( $\Delta E$ ) induced by exchange interaction is in the range of 0.1 – 0.4 meV [7, 17, 18]. The transition or spin-flip time between dark and bright states is temperature-dependent [17, 18] and we assume that,

$$\tau_{db} = \tau_{bd} \times \exp(\Delta E / k_B T), \quad (1)$$

where  $k_B$  is Boltzmann constant and  $T$  is the sample temperature.

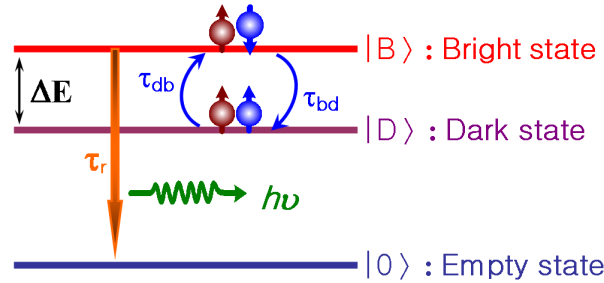


Fig. 4. The theoretical model considering the excitonic bright, dark and empty states.

By considering the exciton transferring between these states and by ignoring the non-radiative recombination process (due to the fact of that the integrated PL intensities keep in  $\pm 10\%$  in the studied temperature range), we can write down the coupled rate equations as follows.

$$\frac{dN_B}{dt} = -\frac{N_B}{\tau_r} - \frac{N_B}{\tau_{bd}} + \frac{N_D}{\tau_{db}} \quad (2a)$$

$$\frac{dN_D}{dt} = -\frac{N_D}{\tau_{db}} + \frac{N_B}{\tau_{bd}} \quad (2b)$$

The variable  $N_B$  ( $N_D$ ) is the time-dependent occupation number in the bright (dark) excitonic state and  $\tau_r$  is the radiative recombination time. Equation (2) has an analytical solution for  $N_B(t)$  in the form,

$$N_B(t) = A_1 \cdot e^{-t/\tau_1} + A_2 \cdot e^{-t/\tau_2} \quad (3)$$

where

$$\frac{1}{\tau_1} = \frac{\tau_{db}\tau_{bd} + \tau_{db}\tau_r + \tau_{bd}\tau_r + \sqrt{-4\tau_{db}\tau_{bd}^2\tau_r + (\tau_{db}\tau_{bd} + \tau_{db}\tau_r + \tau_{bd}\tau_r)^2}}{2\tau_{db}\tau_{bd}\tau_r} \quad (4a)$$

$$\frac{1}{\tau_2} = \frac{\tau_{db}\tau_{bd} + \tau_{db}\tau_r + \tau_{bd}\tau_r - \sqrt{-4\tau_{db}\tau_{bd}^2\tau_r + (\tau_{db}\tau_{bd} + \tau_{db}\tau_r + \tau_{bd}\tau_r)^2}}{2\tau_{db}\tau_{bd}\tau_r} \quad (4b)$$

$$A_1 = \left( \frac{\tau_{db}\tau_{bd} + \tau_{db}\tau_r - \tau_{bd}\tau_r}{2\sqrt{-4\tau_{db}\tau_{bd}^2\tau_r + (\tau_{db}\tau_{bd} + \tau_{db}\tau_r + \tau_{bd}\tau_r)^2}} + \frac{1}{2} \right) \cdot N_B(0) + \frac{-\tau_{bd}\tau_r}{\sqrt{-4\tau_{db}\tau_{bd}^2\tau_r + (\tau_{db}\tau_{bd} + \tau_{db}\tau_r + \tau_{bd}\tau_r)^2}} \cdot N_D(0) \quad (4c)$$

$$A_2 = \left( \frac{-\tau_{db}\tau_{bd} - \tau_{db}\tau_r + \tau_{bd}\tau_r}{2\sqrt{-4\tau_{db}\tau_{bd}^2\tau_r + (\tau_{db}\tau_{bd} + \tau_{db}\tau_r + \tau_{bd}\tau_r)^2}} + \frac{1}{2} \right) \cdot N_B(0) + \frac{\tau_{bd}\tau_r}{\sqrt{-4\tau_{db}\tau_{bd}^2\tau_r + (\tau_{db}\tau_{bd} + \tau_{db}\tau_r + \tau_{bd}\tau_r)^2}} \cdot N_D(0) \quad (4d)$$

The  $N_B(0)$  and  $N_D(0)$  are the initial populations of bright and dark states, respectively. The solution, although analytical, is so complicated. We can simplify it by using the approximation,  $\tau_{db} \cong \tau_{bd} \equiv \tau_s$ . This approximation can be justified with that, at the temperature range of interest ( $T > 30$  K), the exponential factor in Eq. (1) is close to 1 even for  $\Delta E = 0.4$  meV. Accordingly, the solution becomes,

$$\tau_1 = \frac{1}{2}(\tau_s + 2\tau_r - \sqrt{\tau_s^2 + 4\tau_r^2}) \quad (5a)$$

$$\tau_2 = \frac{1}{2}(\tau_s + 2\tau_r + \sqrt{\tau_s^2 + 4\tau_r^2}) \quad (5b)$$

$$A_1 = \left( \frac{\tau_s}{2\sqrt{\tau_s^2 + 4\tau_r^2}} + \frac{1}{2} \right) \cdot N_B(0) + \frac{-\tau_r}{2\sqrt{\tau_s^2 + 4\tau_r^2}} \cdot N_D(0) \quad (5c)$$

$$A_2 = \left( \frac{-\tau_s}{2\sqrt{\tau_s^2 + 4\tau_r^2}} + \frac{1}{2} \right) \cdot N_B(0) + \frac{\tau_r}{2\sqrt{\tau_s^2 + 4\tau_r^2}} \cdot N_D(0) \quad (5d)$$

At very low temperature, the spin-flip time  $\tau_s$  is very long ( $\sim 100$  ns) comparing with the radiative recombination time  $\tau_r$  ( $\sim 1$  ns) but it shortens with increasing temperatures. Typically,  $\tau_r$  would be nearly constant with temperature in this temperature range ( $< 100$  K). Therefore, the only two parameters are  $\tau_s$  and the ratio between  $N_B(0)$  and  $N_D(0)$ , the later one is usually assumed as one (equal populations). In the limiting cases of very large and very

small  $\tau_s$ , the solution gives expected results which have been observed and discussed previously [8,19,20]. That is, when the  $\tau_s$  is very large (small),  $\tau_1 \sim \tau_r$  and  $\tau_2 \sim \tau_s$  ( $\tau_1 \sim 0$  and  $\tau_2 \sim 2\tau_r$ ). However, it is not possible to explain our observations with these limiting cases because the measured decay time is simply too large (the maximum decay time in theory is  $2\tau_r$ ). One possible way out comes from Eq. (5c). If  $A_1$  vanishes, the substitution of the fast decay with the slow one could happen. To make  $A_1$  equal to zero, we need

$$\tau_s = \frac{[N_D(0)/N_B(0)]^2 - 4}{2N_D(0)/N_B(0)} \tau_r \quad (6)$$

This can be true only if  $N_D(0)/N_B(0)$  is larger than 2 because the spin-flip time  $\tau_s$  is always positive. We can place Eq. (6) into Eq. (5b) to obtain the value of  $\tau_2$ , which is the new  $\tau_1$  after the substitution taking place but it is easier to plot them by using the Eqs. (5a) to (5d) with  $\tau_r = 1$  ns, as illustrated in Fig. 5.

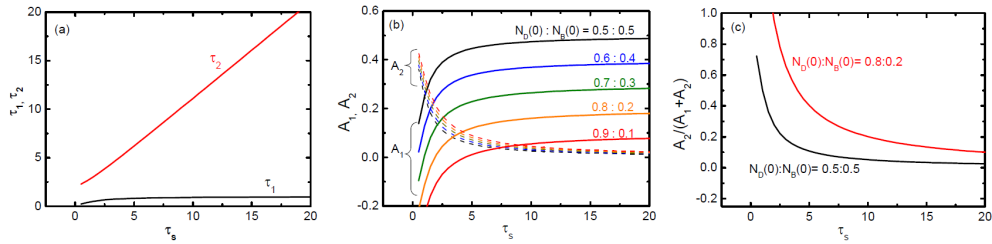


Fig. 5. The theoretical dependence of  $\tau_1$  and  $\tau_2$  (a), their respective coefficients  $A_1$  (solid) and  $A_2$  (dash) (b), and resultant  $A_2$  ratios (c) on spin-flip time  $\tau_s$ . Note that  $\tau_r = 1$  ns is used here.

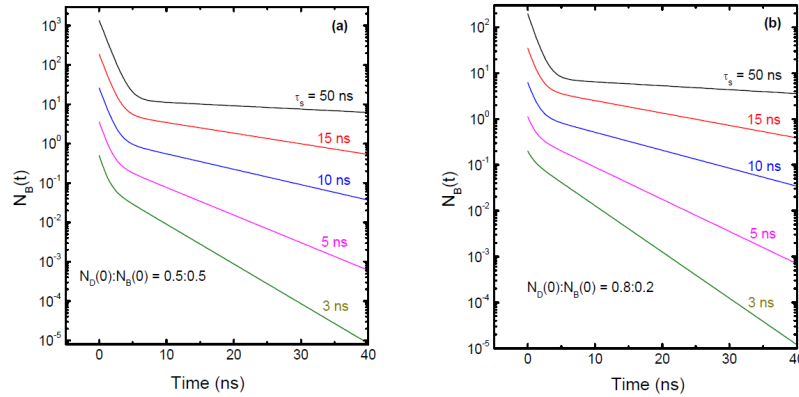


Fig. 6. The theoretical time traces under various spin-flip times for the balanced (a), and imbalanced (b) initial population between dark and bright states.

In Fig. 5(a), we can see that, with decreasing spin-flip time  $\tau_s$  (that is, with increasing temperature), the slow decay time  $\tau_2$  decreases linearly but the fast decay time  $\tau_1$  is nearly unchanged except for  $\tau_s$  getting close to  $\tau_r$ . With various  $N_D(0)/N_B(0)$  ratios, the  $A_1$  and  $A_2$  dependences on  $\tau_s$  are shown in Fig. 5(b). Look at the conventional case  $N_D(0):N_B(0) = 0.5:0.5$  first, for large  $\tau_s$  ( $\gg \tau_r$ ),  $A_1 \sim 0.5$  and  $A_2 \sim 0$ . Only when  $\tau_s \sim \tau_r$ ,  $A_2$  can be larger than  $A_1$ , which is one of the limiting cases discussed above. However, with larger  $N_D(0)/N_B(0)$  ratios, the value  $\tau_s$  making  $A_1$  equal to zero becomes larger. Because the substitution could happen at larger  $\tau_s$ , from Fig. 5(a), a larger  $\tau_2$  (could be much more than the twice of  $\tau_r$ ) is obtained. That is, a larger  $N_D(0)/N_B(0)$  ratio could give a longer decay time when the

substitution occurs. We also plot the corresponding  $A_2$  ratios,  $A_2/(A_1 + A_2)$ , in Fig. 5(c). With imbalanced initial population and decreasing  $\tau_s$ ,  $A_2$  ratio goes to 1 much earlier than the balanced case. In other words, the substitution occurs even when the spin-flip time  $\tau_s$  is larger than but not close to the radiative recombination time  $\tau_r$ . The theoretical time traces in Fig. 6 show even clear pictures for the difference between balanced and imbalanced initial populations. The balanced initial condition in Fig. 6(a) gives a conventional dependence on temperature. At  $\tau_s = 50$  ns, a clear two-component decay is seen. With decreasing  $\tau_s$ , the slow decay ( $\tau_2$ ) fastens but not taking over the fast decay even at  $\tau_s = 3$  ns. Comparing with those in Fig. 6(b), the fast decay part becomes unclear or the substitution occurs when  $\tau_s = 5$  ns or lower. It is worth noting that the theoretical time traces in Fig. 6 resemble those measured ones in Fig. 1 (taken from samples S1 and S3). The dependence of excitation power illustrated in Fig. 3 also becomes reasonable with our analysis. A higher excitation power enhances the probability of biexciton occupation. After the biexciton generates a photon, the left exciton is in the bright state so the  $N_D(0):N_B(0)$  ratio reduces. Lowered  $N_D(0):N_B(0)$  ratios suppress the substitution of the fast decay by the slow one, which is exactly what we see in Fig. 3. In short, the long decay time is caused by not only the shortened spin-flip time but also by the imbalanced initial condition.

### 3.3 Sample dependence

Let us show the TRPL results taken under low excitation power from those six samples listed in Table 1 above. In Fig. 7, the extracted fast decay times  $\tau_1$  and  $A_2$  ratios are plotted against the sample temperatures. In Fig. 7(a), it is clear that the unusual long decay times are obtained with the samples S3 and S4. The longest decay times for samples S3 and S4 are about 5.4 ns and 14 ns, respectively. The corresponding high  $A_2$  ratios in Fig. 7(b), which are about 0.42 and 0.85 for samples S3 and S4, respectively, demonstrate that the long decay times are caused by the replacement of fast decay with the slow one. Interestingly, among the more than 20 studied samples, although there is no correlation between the growth conditions of QDs and the observation of long decay time, the PL ground state energy in the range of 1.20 – 1.26 eV is indeed a necessary (but not sufficient!) condition for seeing unusual behavior. It seems to us that the imbalanced initial condition mentioned previously could only happen in the middle-sized QDs. Therefore, the spin-dependent relaxation process could be more effective in certain sizes of QDs. To study the spin relaxation process from 3-D bulk or 2-D quantum-well states to 0-D QD states needs further either theoretical or experimental works. One possible mechanism is proposed here. When the electron-hole pair is generated in barrier GaAs, the hole could be first captured by the QD due to its faster relaxation time. The captured hole may have influenced the spin relaxation process of electron through spin-spin interaction to enhance the occupation probability of dark states, which results the needed imbalanced initial population. In addition, other factors such as the size-dependent energy difference between dark and bright states [18] and the nuclear spin dynamics [3, 21] could also play a role here but further investigations are certainly needed to clarify this issue.



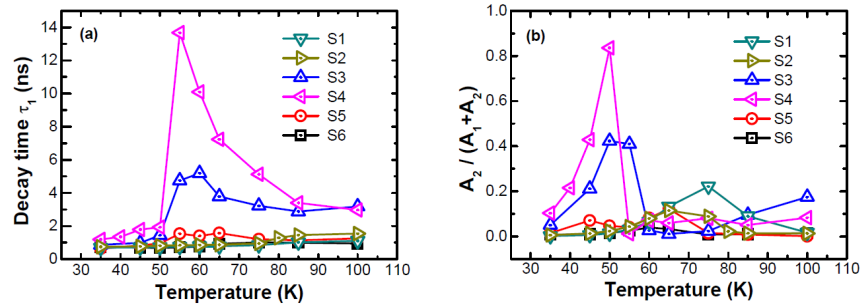


Fig. 7. The measured fast decay times (a) and  $A_2$  ratios (b) from the six samples S1 to S6 at various temperatures.

#### 4. Conclusion

In conclusion, we presented the observation of long-lived exciton in individual InAs QDs, which is caused by the substitution of the fast decay by the slow one as the effective spin-flip times shorten. The general model considering the interplay between dark and bright states and the analytical solution of its rate equation indicates that there are two key factors to make the unusual behavior happen. The first one is a fastened spin-flip time and the second one, which plays a critical role, is the imbalanced initial populations between the dark and bright states. Our work calls for further studies on spin-dependent relaxation process and paves the way to use dark excitons for spin storage at elevated temperatures.

#### Acknowledgment

This work was financially supported by NSC (100-2628-E-009-009) and MOE (ATU program) in Taiwan. The equipment support from CNST at NCTU is appreciated. We thank Profs. C. P. Lee, W. H. Chang, and S. J. Cheng for their inspiring discussions.